21st Australasian Fluid Mechanics Conference
Adelaide, Australia
10-13 December 2018

CFD Studies on the Radial Feeding in High-Speed Vane Pumps

M. Rundo[1] and G. Altare[1]

[1]Department of Energy
Politecnico di Torino, Turin 10129, Italy

Abstract

The filling capability of a positive displacement pump is influenced by the geometry of the suction side. In this study, the effect of the lateral grooves manufactured on the stator of a variable displacement lubricating pump is analysed. The 3D CFD model of the pump developed with the tool PumpLinx® is presented. Different configurations of the stator are analysed. The model has been validated experimentally in terms of steady-state flow-speed characteristics at two different constant displacements. The study has brought to evidence that the increment of the suction flow area by means of additional lateral paths machined on the stator has a detrimental effect on the pump filling. The reason is the increment of the back flow generated by the centrifugal force, which decreases the net flow rate sucked by the variable volume chambers.

Introduction

In positive displacement pumps, the real delivered flow rate differs from the theoretical value due to the fluid leakages. However, another important source of volumetric loss is represented by the incomplete filling of the chambers. Such a condition occurs at high speed and is worsened by the low suction pressure and by the high fluid viscosity. Lubricating pumps [6] for automotive and aeronautical applications are particularly affected by such a problem, being driven at an angular velocity proportional to the engine speed. The phenomenon begins at a critical speed, in correspondence of which the maximum pressure drop available between the chambers and the suction port (1 bar at sea level) is reached. It is desirable that such a critical speed could fall outside the working range of the pump. For a given suction pipe geometry, the only way for reducing the pressure losses is to increase as much as possible the flow area between the variable chambers and the inlet port, since at high speed most of the pressure drop is localized across the port plate. In internal gear and vane pumps, the maximum flow area of the chambers is given by their frontal surface; hence it can be slightly modified by changing the geometric parameters of the rotor. Best results are obtained by reducing the diameter of the rotor [1], in order to decrease the peripheral speed, and by feeding the chambers from both sides [4]. In vane pumps, an additional flow area can be generated on the outer radius of the chambers by decreasing locally the axial height of the stator. However, a possible drawback is the increment of the reverse flow generated by the centrifugal force. Due to the complexity of the flow field, only a 3D CFD simulation can be used as predictive tool for the design of the pump.

The studies on 3D CFD simulations of vane pumps are quite limited and most of them made with the dedicated software PumpLinx [2]. With such a tool Wang et al. [8] studied a pump with a pivoting stator and a direct acting displacement control. Later Frosina et al. [3] simulated a vane pump provided with a piloted displacement control. Finally, the authors of this paper studied a variable displacement pump using an integrated approach involving 0D (homogeneous fluid properties in the control volumes) and 3D models [5]. However, a focused analysis on the axial and radial flow for filling the variable chambers is not present in the open literature.

In this paper, different flow paths for connecting the chambers to the suction volume are contrasted through 3D CFD simulations. It was found that, unlike other pump types, in case of vane pumps with a high diameter/height ratio, the increment of the flow area, above all if obtained through millings on the stator, can give detrimental effects on the volumetric efficiency.

Component description

The reference pump is a 15.3 cc/rev vane type unit with variable displacement. A 3D view of the pump without the cover is presented in figure 1. The rotor is driven directly by the engine crankshaft and houses 9 vanes, whose tip is in sliding contact with the internal track of the stator, mounted with eccentricity with respect to the rotor. The displacement is modified by means of the linear movement of the stator that can slide with respect to the housing, in order to vary the eccentricity with the rotor. The prismatic guides work also as linear actuators with different active surfaces. The details of the displacement control are not reported in this paper, since the study was performed at fixed and imposed eccentricity of the stator.

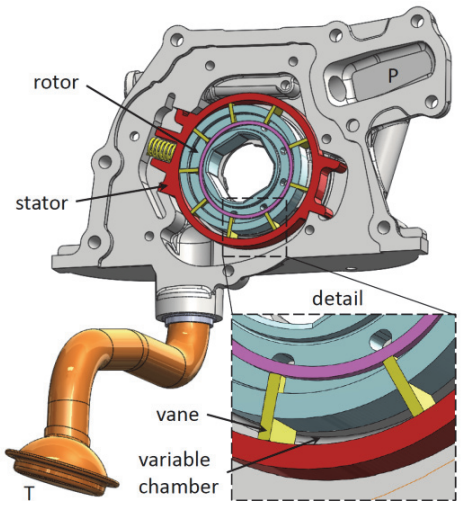

Figure 1. 3D view of the reference pump.

CFD model

The 3D CFD model was built with the commercial software PumpLinx, which allows managing easily moving grids by means of a specific template for vane pumps. The code discretizes the governing equations using the finite volume method and solves the conservation equations of mass and momentum. In the present study, the first order upwind

interpolation scheme was used, while the SIMPLE-S algorithm was employed for the pressure-velocity coupling. More details about the numerical models can be found in [2].

The fluid volume inside the pump was extracted from the CAD geometry, then was divided in subdomains, converted in STL format with SpaceClaim® and finally imported in PumpLinx. In the variable chambers the cells are anchored to the vanes and to the outer diameter of the rotor, while are sliding with respect to the stator. In order to adapt the grid to the variation of the volume, the cells are stretched or shortened in the radial direction. The axial leakages between the rotor and the cover are also taken into account by means of a disc of cells made up of three layers. The mesh independence analysis led to about 800,000 cells. More details about the model can be found in the Ref. [5]. The fluid model *Equilibrium Dissolved Gas* was used for simulating the cavitation and aeration. It evaluates the density of the mixture oil, gas and air as function of the mass fractions and of the equilibrium conditions based on the Henry's law [7]. The simulations were performed at constant eccentricity of the stator. In the boundary conditions, the atmospheric pressure was imposed at the inlet of the suction pipe T, while at the outlet port P a pressure of 3 absolute bar was set.

With reference to figure 2, the analysed configurations are listed in table 1. In the baseline configuration (1), the chambers with axial height H = 12 mm are fed only from the casing side and a milling of the stator with height h1 = 2 mm is machined. The modifications have involved the stator and the cover. In particular, in the configurations 2, 3 and 5, on the cover side there is an additional milling on the stator with height h2. Finally, the configurations 4 and 5 have a modified cover with an additional passage with height h3. The detail of the mesh in the inlet volume is shown in figure 3; the outlines of the variable chambers are also indicated.

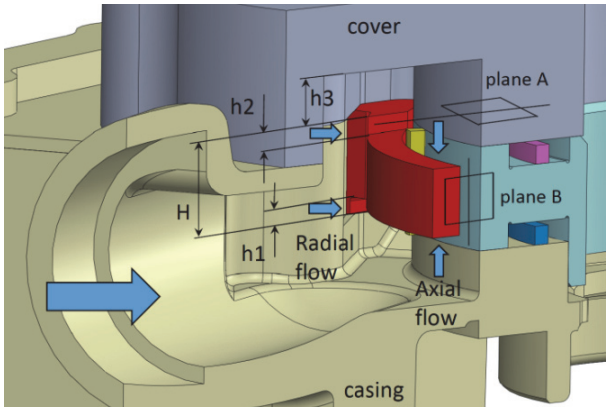

Figure 2. Geometric parameters.

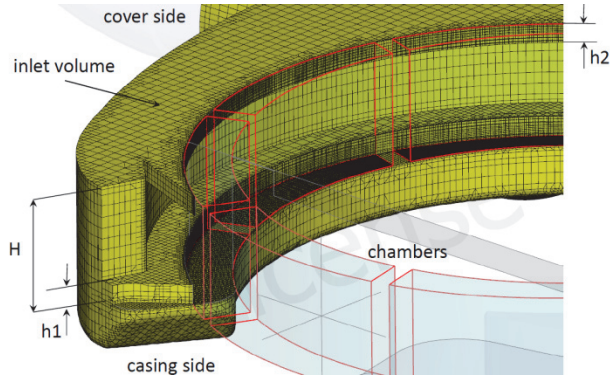

Figure 3. Mesh in the inlet volume in the configuration 3

The simulations were performed at 5200 rpm and 55% of the maximum displacement. This is a reasonable operating condition on the engine, since the pump works at maximum eccentricity only at medium-low speeds. In table 1 the flow rate delivered by the pump is shown. Since the simulations were performed at constant delivery pressure, the leakages are constant; hence the variation of the flow rate is only due to the effect of the incomplete filling.

Config.	h1 (mm)	h2 (mm)	h3 (mm)	Flow rate (L/min)
1	2	0	0	40.1
2	2	1	0	37.4
3	2	2	0	33.2
4	2	0	5	37.4
5	2	2	5	35.4

Table 1. Geometric parameters for each analyzed configuration and corresponding simulated flow rates at 5200 rpm - partial displacement.

Model validation

The CFD model has been validated using the test rig shown in figure 4, where the pump under test is mounted on a support block that houses the shaft driven by a variable speed electric motor (M1). The load is simulated by a proportional throttle valve (R1) that can be controlled in closed loop with a feedback signal coming from a pressure transducer. In this specific case, a pressure transducer GS XPM5, with measuring range 0-20 bar (absolute) and linearity error ± 0.25% F.S. was mounted just outside the delivery port of the pump. The flow rate is measured by a mass flow meter MICROMOTION CMF100M with accuracy on the measured volumetric flow rate of ±0.10% and repeatability ±0.05%.

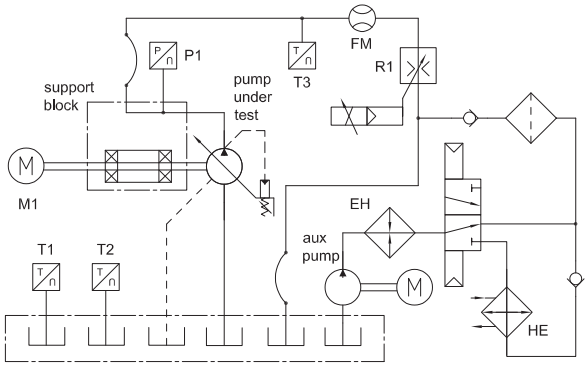

Figure 4. Hydraulic scheme of the test rig.

The pump sucks a synthetic base oil SAE 5W30 from a 30 L reservoir. The density is 837 kg/m^3 and the dynamic viscosity 50 cP at 40 °C. The fluid conditioning system is constituted by a constant speed auxiliary pump, two 5 kW electric heating elements (EH), a water-oil heat exchanger (HE) and a filter. The auxiliary pump takes the oil from the reservoir and delivers the fluid to the return line of the main circuit. A closed loop control system, based on the feedback signal of two PT100 resistance temperature detectors, allows maintaining a constant temperature in the reservoir.

The pump was tested at constant displacement, with the stator mechanically blocked. The tests were performed at constant delivery pressure of 3 absolute bar imposed by the valve R1. The speed of the pump was increased by steps from 1000 rpm up to the region of defective filling. For each speed value the delivery flow rate was measured. The original stator (config. 1) and with the milling with height h1 = 1 mm (config. 2) were tested at maximum displacement up to 4500 rpm. The

baseline configuration was also contrasted with the configuration 3 (h2 = 2 mm) at partial displacement up to almost 6000 rpm.

The comparison between the experimental measurements and the CFD simulations (dots) is reported in figure 5. At medium-low speed a linear relationship between the flow rate and the speed is observed. In fact in these conditions the only volumetric loss is due to the fluid leakages, but since the tests were executed at fixed delivery pressure, such a contribution remains constant as the speed increases. Hence the slope of the characteristic is given by the displacement of the pump. At high speed the flow rate saturates and even slightly decreases: such behaviour is caused by the incomplete filling. In this case only a fraction of the chamber volumes is exploited to generate the oil flow rate, being the remaining volume filled with the gaseous phase.

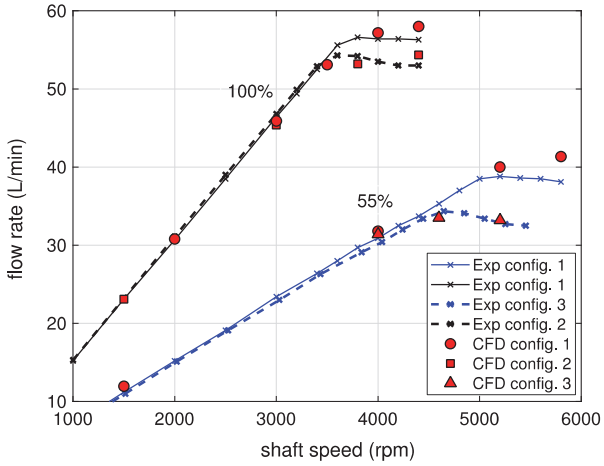

Figure 5. Flow-speed curves at fixed displacement – 100% and 55%.

Discussion

From the point of view of the reduction of the hydraulic resistance from the reservoir to the chambers, the increment of the flow area has always a beneficial effect, above all at high displacement. However the simulated flow rates listed in table 1 show that the feeding of the chambers from both sides has a detrimental effect on the filling. Moreover the presence of the milling on the stator at the cover side worsens significantly the pump suction capability. In order to better understand the reason of such behaviour, the instantaneous flow rate simulated in a generic variable chamber has been analysed. In figure 6 the flow rate entering a chamber as function of the shaft angle is plotted for three configurations.

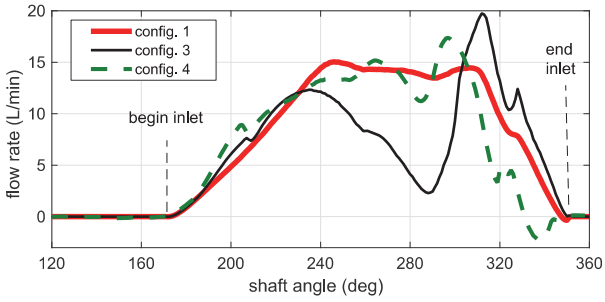

Figure 6. Total flow rate entering a chamber vs. angle.

By comparing the configurations 1 and 4, it is evident that the behaviour is almost the same in the first half of the suction phase, while at the end the ingoing flow rate is significantly lower in spite of the fact that the chamber is fed from both sides. Moreover a negative flow rate is observed in the last part of the suction phase, at about 340 degrees. If the double feeding is obtained through the milling on the stator, instead of on the cover (configuration 3), starting from 240 degrees the net ingoing flow rate decreases dramatically and only at the end of the suction phase a better behaviour with respect to the baseline configuration is observed. Figure 7 shows the comparison between the axial flow (through the frontal surfaces of the chambers) in the configuration 1 and 3, while in figure 8 the radial flows through the millings in the stator are contrasted. From figure 7 it is possible to observe that the flow rate with the configuration 3 is even double in the second part of the suction phase with respect to the baseline. However such a high flow rate is due to the fact that a huge outcoming flow is observed in figure 8 through the milling on the cover side, with a maximum at about 300 degrees.

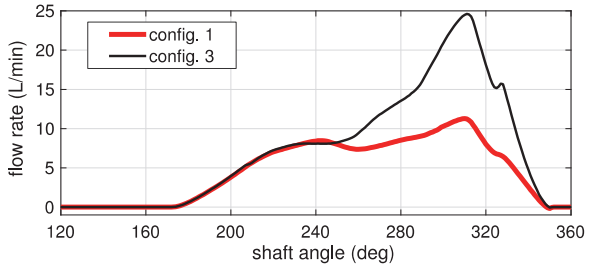

Figure 7. Axial flow rate through the frontal surfaces.

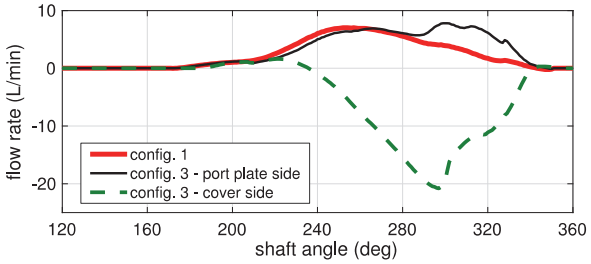

Figure 8. Radial flow rate through the millings on the stator.

It is evident that the additional flow area on the stator with height h2 mainly lets the fluid escape from the chamber, rather than helping it to enter. In the figures 9 and 10 the pressure field and the detail of the velocity field are reported for the configuration 3 at two different shaft angles: 240 and 280 degrees. In particular the figures show a chamber and the inlet volume in correspondence of the plane A, indicated in figure 2, perpendicular to the rotor axis and passing in the middle of the milling with height h2.

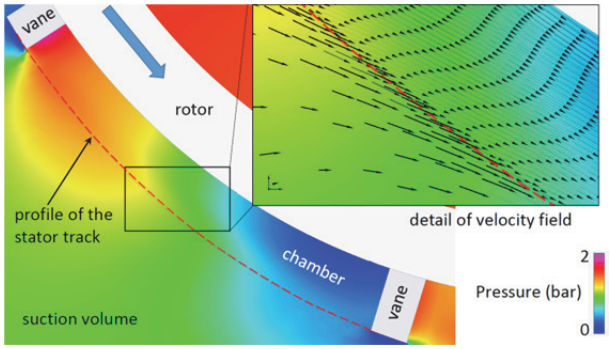

Figure 9. Pressure field in the upper milling - cover side (plane A) at 240 degrees and detail of the velocity field in the configuration 3.

The rotor rotates counterclockwise and it is interesting to notice that there is a non-uniform pressure distribution in the chamber: behind the leading vane the pressure is very close to 0 bar (absolute), while in front of the trailing vane the pressure is about 2 bar, higher than in the suction volume.

In a lumped parameter approach, the pressure in the chamber is considered homogeneous. Since during the suction phase the chamber volume is increasing, its pressure is always lower than in the inlet pipe. The consequence is that any additional increment of the flow area between the chamber and the inlet volume is evaluated as beneficial for improving the filling in a 0D model, regardless of the angular position of the chamber and of the location of the additional passage. However, the fact that in some regions of the chamber the pressure is higher than in the inlet volume implies that a backflow could originate through some portions of the total flow area. This is the reason why, on average, the radial flow rate in the configuration 3 in the cover-side milling is negative. Nevertheless, at 240 degrees the phenomenon is localized; in fact, if the middle of the chamber is considered, the detail of the velocity field in figure 9 shows that the fluid still enters radially the chamber through the upper milling. On the contrary, in the position at 280 degrees, shown in figure 10, the centrifugal force is higher than the effect of the pressure difference and the fluid leaves massively the chamber through the upper slot and a very high negative flow is observed in figure 8.

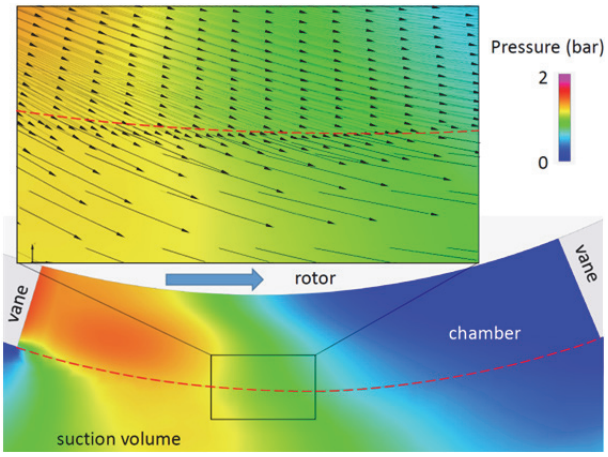

Figure 10. Pressure field in the upper milling (plane A) at 280 degrees and detail of the velocity field in the configuration 3.

For this reason the overall behaviour of the pump worsens in the configuration 2 and even more in the number 3, where the height of the milling is higher. It is well known from the literature than the feeding of the pump also from the cover side has a beneficial effect. However in this machine, even the configuration 4 is less efficient than the baseline. To explain the poor behaviour in the last part of the suction phase observed in figure 6, it is necessary to analyse in figure 11 the axial flow on the plane B passing through the rotor axis.

The two flow rates entering from both sides meet in the middle of the chamber and, due to the centrifugal force, the fluid in the chamber is pushed outwards against the stator track and an internal recirculation originates. If the height H of the stator is quite small, it is possible that at the end of the suction phase, where the chamber derivative is not so high, the fluid could leave the chamber in the region indicated in figure 11. In the configuration 5 the drawback of the upper milling worsens the filling with respect to the configuration 4.

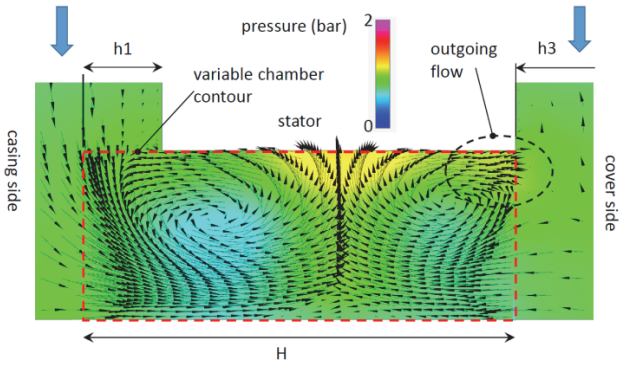

Figure 11. Pressure and velocity fields in a cross section of a chamber (plane B) for the configuration 4 at 340 degrees.

Conclusions

Different ways for feeding the chambers of a vane pump for engine lubrication have been presented. Unlikely other pump types, in the analysed unit the double feeding has a detrimental effect on the volumetric efficiency. Moreover the slot on the stator for radially filling the chambers reduces the net ingoing flow rate. The reason is the effect of the centrifugal force that generates a back flow during the suction phase. Hence the increment of the flow area through additional passages must be carefully evaluated in pumps with a high diameter and a small axial thickness. Future studies will be focused on determining the combination of geometrical parameters discriminating the effect of the increment of the suction flow areas.

References

[1] Altare, G. & Rundo, M., Computational Fluid Dynamics Analysis of Gerotor Lubricating Pumps at High Speed: Geometric Features Influencing the Filling Capability, *ASME J. Fluids Eng.*, **138**(11), 2016.

[2] Ding, H., Visser, F.C., Jiang, Y. & Furmanczyk, M., Demonstration and Validation of a 3D CFD Simulation Tool Predicting Pump Performance and Cavitation for Industrial Applications, *Proceedings of ASME Fluids Engineering Division Summer Meeting*, Vail, USA, 2009.

[3] Frosina, E., Senatore, A., Buono, D. & Olivetti, M., A Tridimensional CFD Analysis of the Oil Pump of an High Performance Engine, *SAE paper 2014-01-1712*, 2014.

[4] Kumar, M.S. & Manonmani, K., Numerical and Experimental Investigation of Lubricating Oil Flow in a Gerotor Pump, *Int. J. Auto. Tech.*, **12**(6), 2011, 903-911.

[5] Rundo, M. & Altare, G., Lumper Parameter and Three-dimensional Computational Fluid Dynamics Simulation of Variable Displacement Vane Pump for Engine Lubrication, *ASME J. Fluids Eng.*, **140**(6), 2018.

[6] Rundo, M. & Nervegna, N., Lubrication Pumps for Internal Combustion Engines: a Review, *Int. J. Fluid Power*, **16**(2), 2015, 59-74.

[7] Singhal, A.K., Athavale, M.H., Li, H. & Jiang, Y., Mathematical Basis and Validation of the Full Cavitation Model, *ASME J. Fluids Eng.*, **124**, 2002, 617-62.

[8] Wang, D., Ding, H., Jiang, Y. & Xiang, X., Numerical Modeling of Vane Oil Pump with Variable Displacement, *SAE Paper 2012-01-0637*, 2012.